agronomy

MDPI

Article

Overexpressing *ZmXTH23* Improves Drought and Salt Tolerance in *Nicotiana benthamiana*

Qianqian Mao [1,†], Fuchao Jiao [1,†], Junhua Li [1,†], Yuhe Pei [1], Qiuyue Xing [1], Jianghao Wang [1], Huijun Guo [2], Jun Li [1], Haoyang Li [3], Nicola Cannon [3], Xianmin Chang [3], Xiyun Song [1] and Xinmei Guo [1,*]

[1] College of Agronomy, Qingdao Agricultural University, Qingdao 266109, China
[2] Institute of Crops Sciences, Chinese Academy of Agricultural Sciences, Beijing 100081, China
[3] School of Agricultural Science and Practice, Royal Agricultural University, Cirencester GL7 6JS, UK
* Correspondence: xinmeiguo@qau.edu.cn
† These authors contributed equally to this work.

Abstract

Maize (*Zea mays* L.), a critical global food crop, suffers severe yield losses from drought and salt stresses. Xyloglucan endotransglucosylase/hydrolases (XTHs) are cell wall-modifying enzymes regulating plant growth and abiotic stress responses, but the role of -*ZmXTH23* in drought and salt tolerance remains unclear. Here, we heterologously expressed *ZmXTH23* in *Nicotiana benthamiana* (*N. benthamiana*) and confirmed its extracellular localization. *ZmXTH23*-overexpressing (OE) lines showed significantly increased plant height, root length, and shoot fresh weight under normal conditions. Under 350 mM NaCl or drought stress, the OE lines exhibited enhanced tolerance, with less leaf wilting, higher biomass, and larger leaf area. Physiologically, the OE lines had higher peroxidase (POD) and superoxide dismutase (SOD) activities and relative water content (RWC), but lower malondialdehyde (MDA) content. Additionally, OE seeds maintained ≥50% germination under 120 mM NaCl (WT: 0%) and nearly 100% under 200 mM mannitol. *ZmXTH23* improves drought and salt tolerance in *N. benthamiana* by upregulating antioxidant enzymes and enhancing water retention, making it a promising candidate for maize stress-resistance breeding.

Keywords: *ZmXTH23*; stress resistance; plant growth; *Nicotiana benthamiana*; cell wall modification

1. Introduction

Maize (*Zea mays* L.) is one of the three principal global food crops, yet its productivity is increasingly compromised by climate change. A rise of 1 °C in global mean temperature has been shown to reduce maize yield by 7.4% [1]. Notably, around 70% of maize cultivation occurs in arid and semi-arid regions where an estimated 30 million hectares of farmland are affected by salinization. Consequently, salt stress represents an important constraint on maize yield potential [2]. In addition, water deficit adversely affects maize development across all phenological stages, with the most pronounced impact occurring during seedling and reproductive phases, particularly during flowering [3].

Maize is highly susceptible to abiotic stresses, particularly drought [4] and salinity [5], which impair growth and productivity. These environmental stresses induce alterations in the composition and structure of plant cell walls [6]. Under drought stress, the expression and activity of cell wall-modifying proteins, such as XTHs (xyloglucan endotransglucosylase/hydrolases), β-glucanases, and expansins, are modulated. These proteins facilitate

Academic Editor: Federica Zanetti

Received: 25 April 2026
Revised: 28 June 2026
Accepted: 29 June 2026
Published: 2 July 2026

turgor-driven cell expansion via controlled relaxation of cell wall polysaccharides, a process that enables the continued growth of cells and organs despite adverse water availability [7]. Xyloglucan, a predominant hemicellulose component, plays a critical role in cell wall structure by interacting with cellulose to form a cohesive matrix [8]. It also serves as a substrate for xyloglucan-modifying enzymes known as XTHs, which include endohydrolase (XEH) and Xyloglucan endotransglycosylase (XET). XEH catalyzes the hydrolysis of β-1,4-glycosidic bonds in xyloglucan chains, whereas XET transfers xyloglucan fragments between molecules [9]. Through these activities, XTHs contribute to dynamic modulation of the cell wall, thereby influencing plant responses to abiotic stress [10].

The *xyloglucan endotransglucosylase/hydrolases* (*XTH*) gene family, classified within the glycoside hydrolase family 16 (GH16), is polygenic and exhibits species-specific variations in gene number. For example, rice contains 29 *XTH* genes, *Arabidopsis* 33, wheat 57, tobacco 56, soybean 61, sorghum 35, and maize 31 [11]. Although XTHs are not essential for cell expansion, they play critical roles in plant responses to biotic and abiotic stresses [11]. Functional studies have demonstrated the involvement of specific *XTH* genes in stress adaptation. For example, in *Arabidopsis*, compared to the wild-type Col-0, overexpression of *XTH22* results in increased sensitivity to boron deficiency, whereas *xth22* knockout lines exhibit greater tolerance. Under low boron conditions, *XTH22* upregulation alters the ratio of chelator-soluble to alkali-soluble pectin and reduces the degree of pectin methylesterification [12]. Similarly, the *xth19* mutant displays reduced freezing tolerance compared to the wild-type Col-0 after cold and sub-zero acclimation, a phenotype associated with changes in cell wall composition and structure [13]. In rice, overexpressing *OsXTH19*, a gene encoding a xyloglucan endohydrolase (XEH), leads to reduced xyloglucan levels, decreased aluminum accumulation, and enhanced root growth under aluminum stress [14]. *TaXTH17*, which is localized to the secretory pathway and cell wall, has been found to negatively regulate plant resistance to both salt and drought stress in heterologous systems and in wheat itself [15].

Within the maize genome, 31 *ZmXTH* genes have been identified; among them, *ZmXTH23* is involved in growth and stress responses [11]. In our earlier studies, we analyzed a large-grain mutant, named *tc19*, at the morphological and transcriptome levels corresponding to days after pollination (DAP). *XTH* was more highly expressed in *tc19* than in Chang7-2 (WT) [16], and *ZmXTH23*, which is highly expressed in maize stems, enhanced salt and drought tolerance when expressed in *Escherichia coli* (unpublished data). XTH is a conserved protein family, present across diverse species ranging from bacteria such as *E. coli* to higher plants. Bioinformatics analysis has predicted *ZmXTH23* as a promising functional candidate gene for regulating drought and salt tolerance. The present study aimed to investigate the function of *ZmXTH23* in regulating growth and stress responses in *N. benthamiana*, thereby providing mechanistic insights and evaluating its potential utility for improving stress resilience in maize.

2. Materials and Methods

2.1. Plant Materials and Growth Conditions

N. benthamiana seeds were surface-sterilized by immersion in 75% (*v*/*v*) ethanol for 1 min and 2% (*v*/*v*) sodium hypochlorite (NaClO) for 7 min. The seeds were then rinsed five times in deionized water and germinated on Murashige and Skoog (MS) medium (pH 5.8) in controlled conditions of 25 ± 1 °C, a 16 h light/8 h dark photoperiod, and a light intensity of 120 μmol·m^{-2}·s^{-1}. After ten days, the seedlings were transplanted into sterilized soil consisting of peat and vermiculite in a 3:1 (*v*/*v*) ratio. The plants were then cultivated in a greenhouse under the same temperature and photoperiod conditions.

Analytical-grade chemicals and solvents, including methanol, NaClO, MS medium, were purchased from Shanghai Chemical Reagents Co., Ltd. (Shanghai, China).

2.2. Bioinformatics Analysis

The amino acid sequence of *ZmXTH23* was analyzed using the online tool ProtParam (https://web.expasy.org/protparam/, accessed onn 24 April 2026). Subcellular localization prediction and conserved domain analysis using databases such as NCBI and MEME Suite revealed the structural characteristics and subcellular distribution features of the target protein.

2.3. RNA Extraction and cDNA Synthesis

Total RNA was extracted from *N. benthamiana* leaves using the TAKARA RNA Purification Kit (Cat. No. 9767, TAKARA Bioengineering Co., Ltd., Beijing, China), following the manufacturer's instructions. RNA concentration and purity were assessed using a NanoDrop 2000 spectrophotometer (Thermo Fisher Scientific, DE, USA), with acceptable A_{260}/A_{280} ratios ranging from 1.8 to 2.0. First-strand complementary DNA (cDNA) was synthesized using the HiScript III 1st Strand cDNA Synthesis Kit (Cat. No. R312-01, Vazyme Biotech Co., Ltd., Nanjing, China), according to the manufacturer's protocol. The reaction conditions were 37 °C for 15 min, 85 °C for 5 s, and storage at 4 °C until further use. RNA extraction and cDNA synthesis from maize used the same procedures as described for *N. benthamiana*.

2.4. Construction of Plant Expression Vector

The full-length coding sequence of *ZmXTH23* was amplified from maize cDNA using primers containing *Xba* I and *Bam*H I restriction sites (Table 1). The PCR product was purified with the FastPure Gel DNA Extraction Kit (Cat. No. DC301-01, Vazyme, Nanjing, China) and cloned into pMD19-T (Cat. No. 6019, TAKARA, Kusatsu, Japan) after double digestion with *Xba* I (Cat. No. 1093A, TAKARA, Kusatsu, Japan) and *Bam*H I (Cat. No. 1010A, TAKARA, Kusatsu, Japan). The verified *ZmXTH23* fragment was excised from pMD19-T using *Bam*H I (Cat. No. 1010A, TAKARA, Kusatsu, Japan) and *Xba* I (Cat. No. 1093A, TAKARA, Kusatsu, Japan), and then subcloned into the modified pCAMBIA1300 (pCAMBIA1300-CaMV 35S::MCS-Tnos- CaMV 35S::HygR vector (hygromycin resistance), predigested with *Bam*H I and *Xba* I (Figures S1 and S2). Both restriction sites were present within the multiple cloning sites of the modified pCAMBIA1300, allowing directional insertion of the *ZmXTH23* coding sequence under the control of the CaMV 35S promoter. The resulting recombinant vector pCAMBIA1300-CaMV 35S*::ZmXTH23* was introduced into *Agrobacterium tumefaciens* LBA4404 (Cat. No. AC1001, Weidi Biotechnology Co., Ltd., Shanghai, China) by chemical transformation.

Table 1. Primer sequences used in this study.

Primer	Sequence
ZmXTH23-Xba I-F	gagaacacgggggactctagaATGGCGACGTCGTCTCGTC
*ZmXTH23-Bam*H I-R	ttcgagctcactagtggatccCTACTGCATGGAGCACTCGGC
Hyg-F	ATGAAAAAGCCTGAACTCACCG
Hyg-R	TTATTTGTCTACGTCCCGTCGG
ZmXTH23-qF	GCGACGTCGTCTCGTCATC
ZmXTH23-qR	GAGCACTCGGCTTCTTCTCG
β-actin-F	TGGCATCACACTTTCTACAATG
β-actin-R	GGTGGTGGTGAAGCTGTAAC

2.5. Agrobacterium-Mediated Transformation of N. benthamiana

A. tumefaciens LBA4404 carrying pCAMBIA1300-CaMV 35S::ZmXTH23 was cultured overnight in LB medium with 50 μg/mL kanamycin and 50 μg/mL rifampicin at 28 °C. The cells were harvested and resuspended in infiltration buffer (10 mM $MgCl_2$, 10 mM MES, 200 μM acetosyringone, pH 5.6) to an OD_{600} of 0.6–0.8. Leaf disc transformation was performed as described in [17]. Leaves from 4-week-old plants were cut into 1 cm^2 discs, immersed in bacterial suspension for 10 min, blotted dry, and incubated on MS medium supplemented with 0.1 mg/L 6-benzylaminopurine (6-BA) and 0.01 mg/L naphthaleneacetic acid (NAA) in the dark at 25 °C for 2 days. The discs were then transferred to selection medium (MS + 0.1 mg/L 6-BA + 0.01 mg/L NAA + 50 μg/mL hygromycin + 250 μg/mL cefotaxime) and sub-cultured every 2 weeks. Regenerated T_0 plants were transplanted to soil (Figure S3), and T_3 homozygous lines (OE1, OE2, and OE4) were used for all experiments.

2.6. Genotyping and qRT-PCR Analysis

Genomic DNA was extracted by the CTAB method [18]. PCR genotyping was performed using primers for *ZmXTH23* and the hygromycin resistance gene (Hyg) (Table 1). For qRT-PCR, total RNA from T_3 lines was extracted and reverse-transcribed, and qRT-PCR was performed with ChamQ SYBR qPCR Master Mix (Cat. No. Q311-02, Vazyme) on a CFX96 Real-Time PCR System (Bio-Rad, Hercules, CA, USA). The *N. benthamiana* β-actin gene (GenBank: DQ345959) served as the internal control. The relative expression was calculated using the $2^{-\Delta\Delta Ct}$ method [19]. Three biological replicates were used.

2.7. Subcellular Localization of ZmXTH23

The coding sequence of *ZmXTH23* (without the stop codon) was cloned into the pCAMBIA1302 to generate pCAMBIA1302-CaMV35S::*ZmXTH23-mgfp5*. The recombinant vector, or pCAMBIA1302, was transformed into *A. tumefaciens* GV3101. Bacterial suspensions (OD_{600} = 0.5) were infiltrated into 4-week-old *N. benthamiana* leaves. The plants were grown in the dark for 24 h and then transferred to standard conditions for 24–36 h. GFP fluorescence was visualized with a Confocal Laser Scanning Microscope (CLSM) (TCS SP5 II, Leica Microsystems GmbH, Wetzlar, Germany); excitation: 488 nm and emission: 500–550 nm.

2.8. Phenotypic Analysis Under Normal Conditions

Seeds from the wild-type (WT) and OE lines were germinated on MS medium. After ten days, the seedlings were transferred to soil and grown for one month. Morphological traits (plant height, stem diameter, leaf length, leaf width, leaf area, shoot fresh weight, root fresh weight, and root length) were measured using a ruler, digital calipers, and a leaf area meter (LI-3000C, LI-COR, Lincoln, NE, USA). Fifteen biological replicates per line were evaluated.

2.9. Seed Germination Assay Under Stress

Surface-sterilized seeds were sown on MS medium (control), MS + 120 mM NaCl (salt stress), and MS + 200 mM mannitol (osmotic stress). Each treatment had three replicates of 20 seeds each. Germination (radicle emergence $\geq$ 2 mm) was scored after 7 days.

2.10. Stress Treatment and Physiological Measurements

2.10.1. Salt Stress

One-month-old plants (n = 5 per line) were irrigated with 350 mM NaCl solution (applied as a single shock at the beginning of the treatment, followed by repeat irrigation every 2 days to maintain soil salinity) for 7 days. Control plants received tap water. Pots (diameter 15 cm, height 12 cm) had drainage holes to avoid waterlogging.

2.10.2. Drought Stress

Two models were used:

(1) PEG6000-simulated drought: Plants were irrigated with 200 mL of 20% (*w*/*v*) PEG6000 solution every 2 days for 7 days. PEG6000 was used for adult plant drought simulation because it mimics the osmotic effects of soil water deficit without being absorbed by plant roots, allowing precise control of water potential.
(2) Natural drought: Watering was withheld for 7 days to induce physiological drought stress.

(Control: maintained under a normal irrigation schedule).

Following these treatments, phenotypic traits were measured as previously described. The application of NaCl and PEG6000 for 7 days was established based on preliminary phenotypic screening. This concentration acts as an acute and severe stress threshold that is sufficient to induce distinct morpho-physiological symptoms (e.g., severe wilting and loss of turgor) in wild-type *N. benthamiana* without causing immediate lethality during the observation window.

2.10.3. Physiological Assays

Relative Water Content (RWC): Fresh leaf samples (0.5 g, fresh weight (Wf)) were soaked in distilled water for 8 h to obtain turgid weight (Wt), then dried at 75 °C until a constant weight was achieved to determine (Wd).

The relative water content was calculated using the following formula [15]:

$$\text{RWC (\%)} = [(\text{Wf} - \text{Wd})/(\text{Wt} - \text{Wd})] \times 100$$

Malondialdehyde (MDA): MDA levels were measured as an indicator of lipid peroxidation. Fresh leaf tissue (1 g) was ground in 10% (*w*/*v*) trichloroacetic acid (TCA) and centrifuged at 4000× *g* for 10 min. A 2 mL aliquot of supernatant was mixed with 2 mL of 0.67% (*w*/*v*) thiobarbituric acid and boiled for 30 min. After cooling, absorbance was measured at 450 nm, 532 nm, and 600 nm, using a spectrophotometer. The MDA content is expressed as (μmol/g Wf) = $[6.45 \times (A_{532} - A_{600}) - 0.56 \times A_{450}] \times V/W$, where A represents absorbance at the specified wavelength, V is the total volume of extract, and W is the fresh weight of the sample [20].

Antioxidant enzymes: POD activity was assayed using a commercial kit (Cat. No. BC0095, Solarbio Science & Technology Co., Ltd., Beijing, China) per the manufacturer's protocol, and the absorbance was recorded at 470 nm. Superoxide dismutase (SOD) activity was quantified using the standard Nitroblue tetrazolium (NBT) photoreduction method, as described by Giannopolitis and Ries [21]. Briefly, the reaction mixture contained 50 mM phosphate buffer (pH 7.8), 13 mM methionine, 75 μM NBT, 2 μM riboflavin, 0.1 mM EDTA, and an appropriate volume of crude enzyme extract. One unit (U) of SOD activity was defined as the amount of enzyme required to cause 50% inhibition of the maximal NBT photoreduction. The absorbance was recorded at 560 nm using a spectrophotometer.

2.11. Statistical Analysis

The data were analyzed using SPSS 26.0 (IBM, New York, NY, USA). Significant differences between the WT and OE lines were determined by one-way analysis of variance (ANOVA), followed by Duncan's multiple comparison test for post hoc comparisons with statistical significance. A single asterisk indicates a significant difference between the OE lines and wild-type ($p < 0.05$), while double asterisks indicate an extremely significant difference ($p < 0.01$). The results are presented as the mean ± standard deviation (SD) based on at least three biological replicates per treatment.

3. Results

3.1. Bioinformatics and Sequence Analysis of ZmXTH23

Subcellular localization prediction and conserved domain analysis using databases such as ProtParam, NCBI, and MEME Suite revealed that ZmXTH23 contains the highly conserved Glyco_hydro_16 domain (PF00722) and XET_C domain (PF06955), both of which are typical characteristics of the XTH protein family (Figure 1A). Motif composition analysis further identified two conserved motifs in *ZmXTH23*, consistent with the features of XET-type XTHs and aligning with its predicted xyloglucan endotransglycosylase (XET) activity (Figure 1B). Phylogenetic analysis demonstrated that *ZmXTH23* clusters closely with well-characterized abiotic stress-responsive homologs in *Arabidopsis*, such as *AtXTH23* (Figure 1C) [22]. Furthermore, promoter region analysis identified abundant stress-related *cis*-acting regulatory elements (e.g., ABRE and DRE) (Figure 1D), positioning *ZmXTH23* as a promising functional candidate for regulating drought and salt tolerance in this study [23].

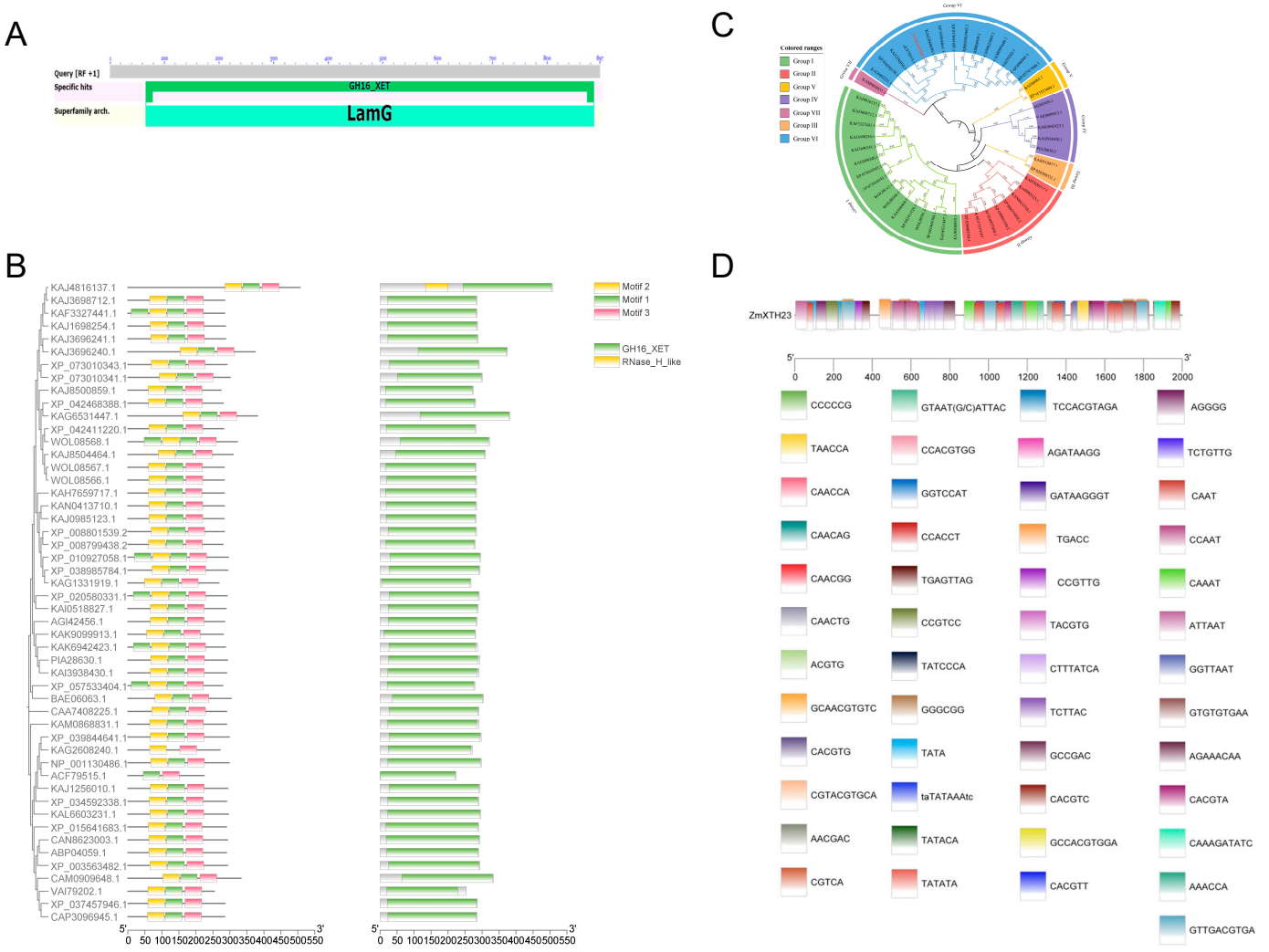

Figure 1. Bioinformatics analysis of the *ZmXTH23* gene. (**A**) Conserved domain analysis, (**B**) the motif and conserved domains, (**C**) homologous phylogenetic tree analysis, and (**D**) prediction of cis-acting elements in the promoter of the *ZmXTH23* gene. Gene of interest are marked in red, while other homologous genes are shown in black.

3.2. The Subcellular Localization of ZmXTH23

Bioinformatic prediction using CELLO suggested that *ZmXTH23* is an extracellular protein. The transient expression of ZmXTH23-GFP in *N. benthamiana* leaves showed a

fluorescent signal restricted to the cell periphery (apoplast), whereas free GFP diffused throughout the entire cell (Figure 2). This indicates that *ZmXTH23* is localized on the cell surface and that its presence in the extracellular matrix is suggested.

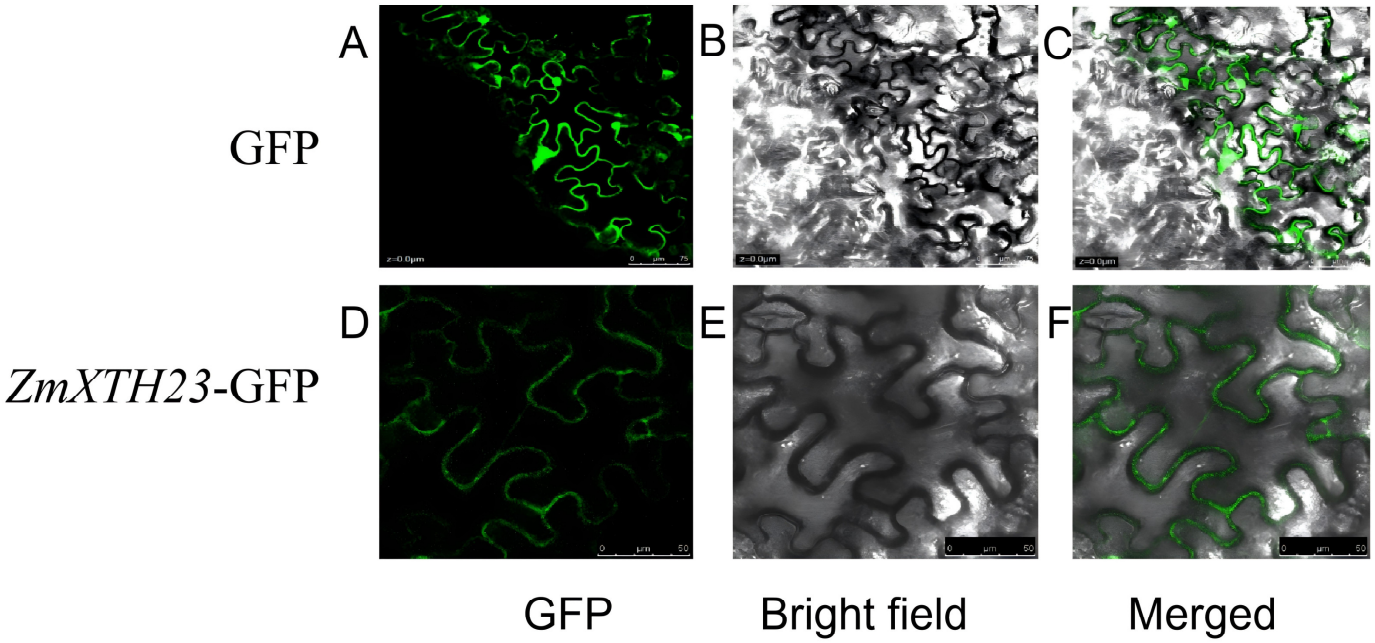

Figure 2. Subcellular localization of *ZmXTH23* in *N. benthamiana* leaves. (**A**–**C**) GFP control: (**A**) GFP fluorescence, (**B**) bright field, and (**C**) merged. (**D**–**F**) ZmXTH23-GFP fusion protein: (**D**) GFP fluorescence, (**E**) bright field, and (**F**) merged. Scale bar = 20 μm.

3.3. Expression Levels of ZmXTH23 in Transgenic Lines

Tobacco seedlings screened with hygromycin were collected for DNA extraction to conduct molecular identification of T_0-positive transgenic lines. As shown in Figure 3A, a total of five T_0 ZmXTH23-positive seedlings were obtained, all of which were successfully transformed. Three positive transgenic plants were selected and designated as OE1, OE2, and OE4; these three overexpression lines, together with wild-type tobacco, were used as materials for subsequent experiments. Total RNA was extracted from leaf tissues of T_3 *ZmXTH23* transgenic lines and wild-type plants, and qRT-PCR analysis revealed that *ZmXTH23* transcript levels were significantly higher in the OE1, OE2, and OE4 lines compared with the WT plants, which had no detectable expression (Figure 3B). OE1, OE2, and OE4 showed 2700-fold, 2600-fold, and 800-fold overexpression compared to the WT, respectively.

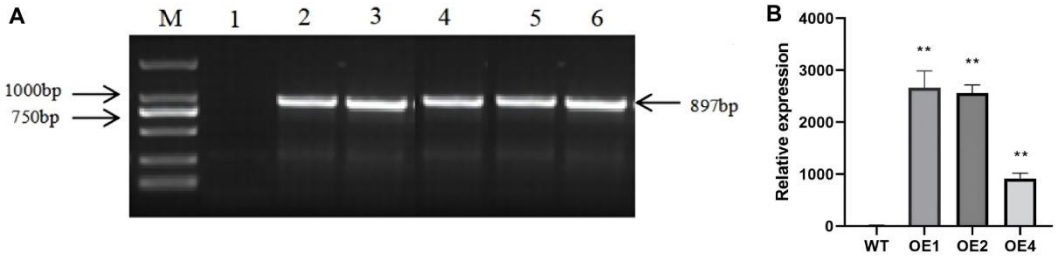

Figure 3. PCR amplification results of T_0 transgenic seedlings (**A**) and qRT-PCR analysis of *ZmXTH23* expression in WT and T_3 OE lines (**B**). M: DL 2000 DNA marker (Takara), 1: wild-type *N. benthamiana*, and 2–6: PCR amplification results of T_0 transgenic seedlings. Relative expression normalized to β-actin. Data are means ± SD (n = 5). ** $p < 0.01$.

3.4. *ZmXTH23* Promotes *N. benthamiana* Growth Under Normal Conditions

The one-month-old OE lines exhibited significantly greater plant height (4.6–6.5% increase) and shoot fresh weight (17–20% increase) compared to the WT (Figure 4A,B). Root length was also increased in OE1 and OE4 (by 16% and 20%, respectively; Figure 4C), while root fresh weight did not differ significantly (Figure 4D). These results indicate that *ZmXTH23* overexpression enhances specific growth parameters under non-stress conditions.

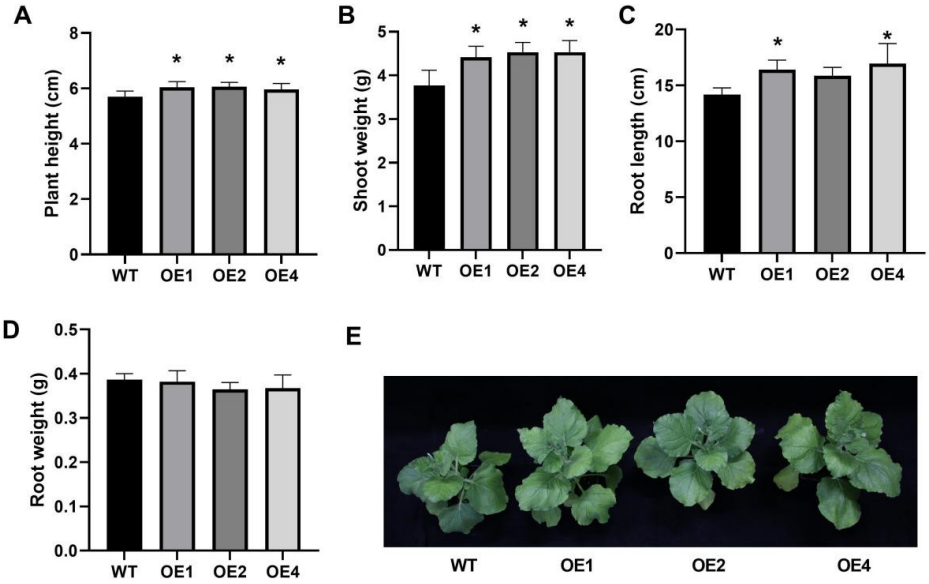

Figure 4. Phenotypic traits of WT- and *ZmXTH23*-overexpressing (OE) *N. benthamiana* lines under normal growth conditions (1-month-old plants). (**A**) Plant height, (**B**) shoot weight, (**C**) root length, (**D**) root weight, and (**E**) phenotype. Data are means ± SD (n = 5). * $p < 0.05$.

3.5. *ZmXTH23* Overexpression Enhances Salt and Drought Tolerance During Seed Germination

Under the normal MS medium, all lines exhibited a 100% germination rate. When treated with 120 mM NaCl, the WT seeds failed to germinate completely (0% germination), whereas the OE lines maintained ≥50% germination rates (Figure 5C,D). Under 200 mM mannitol-induced drought stress (osmotic stress), the WT germination rate was severely reduced (about 15%), while the OE lines reached nearly 100% germination (Figure 5E,F). Thus, all three ZmXTH23-OE lines possessed markedly enhanced salt and drought tolerance during seed germination. *ZmXTH23* enhances seed resistance to both salt and drought stresses at the germination stage in *N. benthamiana*.

3.6. *ZmXTH23* Enhances Salt Stress Tolerance in *N. benthamiana*

To investigate the role of *ZmXTH23* under salt stress, the one-month-old wild-type *N benthamiana* (WT) and *ZmXTH23*-transgenic overexpressing (OE) lines were subjected to salt stress with 350 mmol/L NaCl every 2 days for seven days. Prior to treatment, both the WT and OE lines exhibited normal growth.

After salt exposure (350 mM NaCl treatment), the WT displayed more pronounced leaf wilting, whereas the OE lines showed visibly reduced symptoms (Figure 6A). Statistical analysis revealed that the OE lines had significantly higher shoot weight ($p < 0.05$) and leaf area ($p < 0.05$; Figure 6B,C) compared with the WT plants. Physiological measurements indicated that the OE lines had higher relative water content, lower MDA content, and higher SOD activity, suggesting reduced oxidation damage ($p < 0.05$; Figure 6D–F). These findings demonstrate that *ZmXTH23* overexpression enhances salt stress tolerance in

N. benthamiana, contributing to improved growth and physiological resilience under saline conditions.

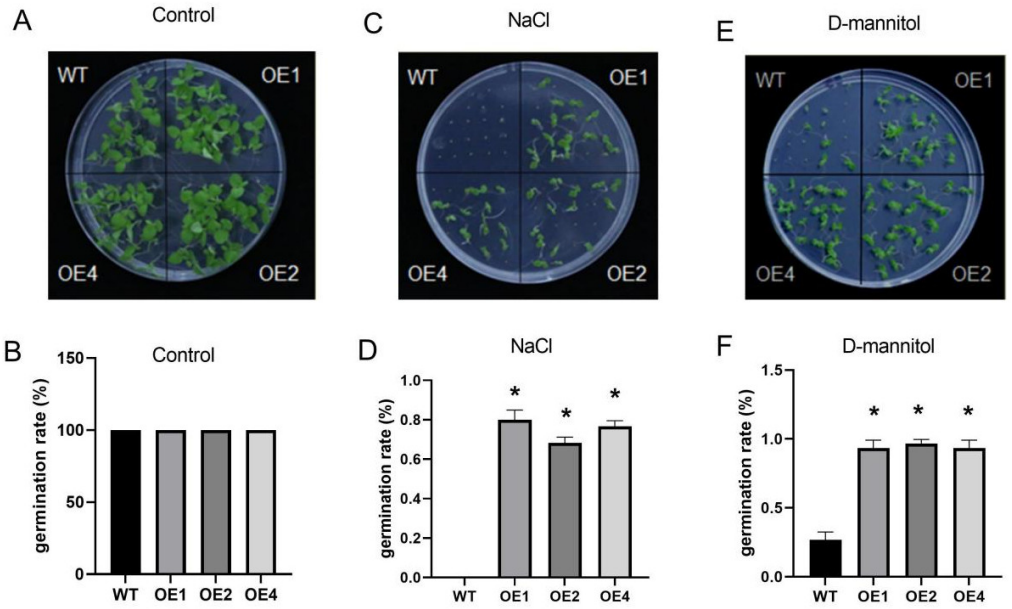

Figure 5. Seed germination of WT and OE lines under normal and stress conditions. (**A**,**B**): Control, MS medium; (**C**,**D**): salt treatment, 120 mM NaCl; and (**E**,**F**): drought treatment, 200 mM D-mannitol. Data are means ± SD (n = 5). * $p < 0.05$.

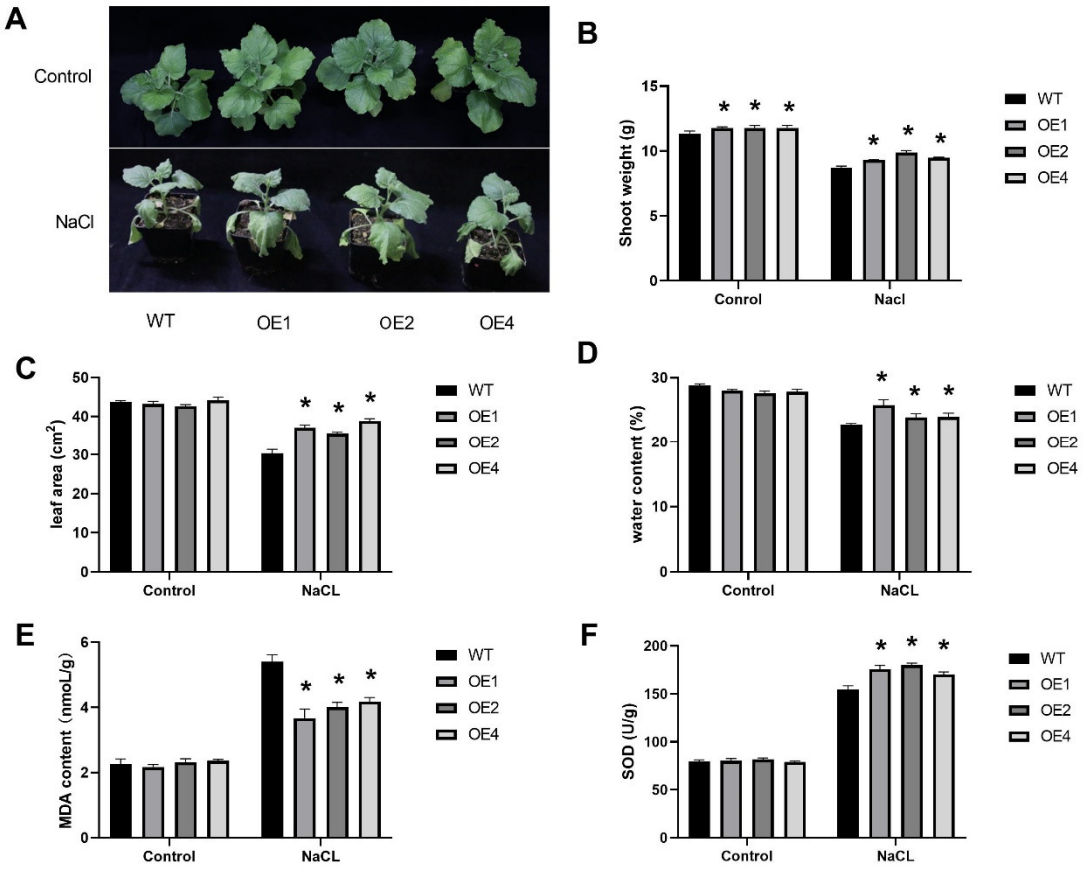

Figure 6. Phenotypic and physiological responses of WT and *ZmXTH23*-overexpressing (OE) *N. benthamiana* lines following 7 days of salt stress (350 mM NaCl). (**A**) Phenotype, (**B**) shoot weight, (**C**) leaf area, (**D**) relative water content, (**E**) MDA content, and (**F**) SOD activity. Data are means ± SD (n = 5). * $p < 0.05$.

3.7. ZmXTH23 Overexpression Enhances Drought Stress Tolerance

3.7.1. PEG6000-Simulated Drought

To investigate the role of *ZmXTH23* under drought stress, the one-month-old wild-type *N. benthamiana* (WT) and *ZmXTH23*-transgenic (OE) lines were treated with 20% PEG6000 every 2 days for 7 days to simulate drought conditions.

Compared to the WT plants, the OE lines exhibited delayed leaf wilting, particularly in the upper leaves, compared with the WT (Figure 7A). The OE lines had significantly greater plant height, root weight, shoot weight, and leaf area ($p < 0.05$; Figure 7B–E). In addition, the OE lines demonstrated superior physiological performance, including lower MDA content and higher POD and SOD activities ($p < 0.05$; Figure 7F–H), indicating reduced oxidative stress. Together, these results suggest that *ZmXTH23* overexpression enhances drought stress tolerance in *N. benthamiana* by promoting and mitigating stress-induced physiological damage.

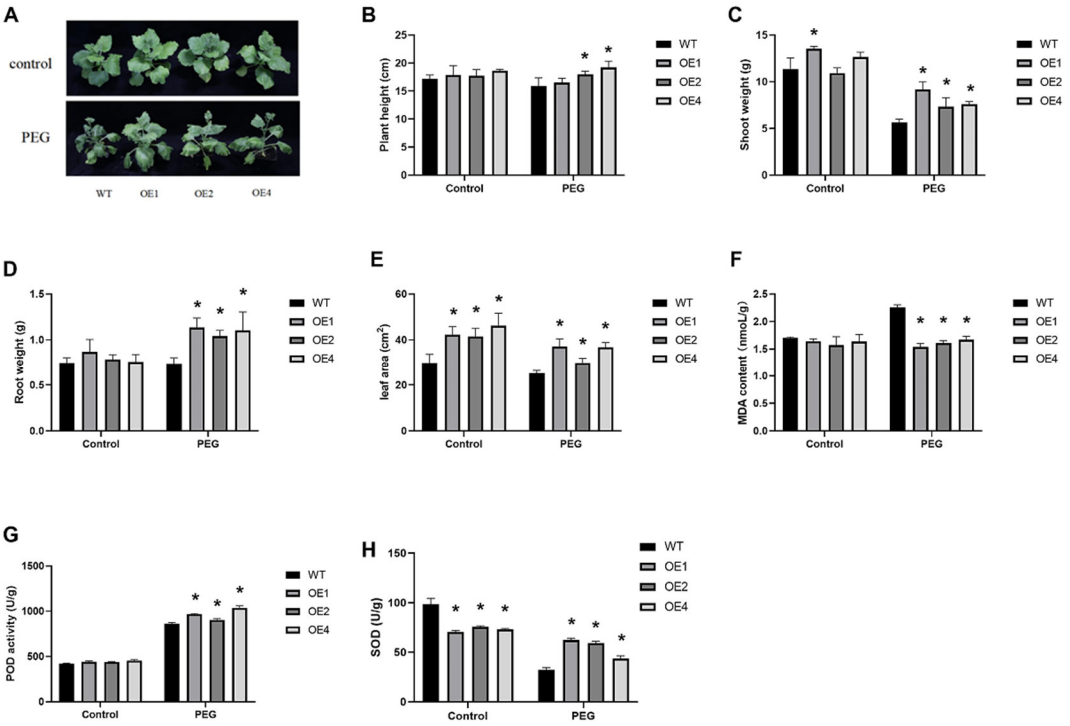

Figure 7. Phenotypic and physiological responses of WT and OE lines after 7 days of 20% PEG6000-simulated drought stress. (**A**) Phenotype, (**B**) plant height, (**C**) shoot weight, (**D**) root weight, (**E**) leaf area, (**F**) MDA content, (**G**) POD activity, and (**H**) SOD activity. Data are mean ± SD ($n = 5$). * $p < 0.05$.

3.7.2. Natural Drought

To investigate the phenotypic response to drought stress, the one-month-old transgenic OE and wild-type *N. benthamiana* plants were subjected to seven days of natural drought stress. Prior to treatment, all of the plants exhibited normal growth.

Following drought exposure, the OE lines showed noticeably less leaf wilting and grew larger than the WT line (Figure 8A). The OE lines had significantly greater plant height, fresh shoot weight, fresh root weight, and leaf area ($p < 0.05$; Figure 8B–E). The physiological assessment showed lower MDA content and higher POD and SOD activity ($p < 0.05$; Figure 8F–H), indicating enhanced oxidative stress response. These findings demonstrate that *ZmXTH23* overexpression improves drought tolerance in *N. benthamiana* by promoting growth and enhancing physiological resilience under water-stressed conditions.

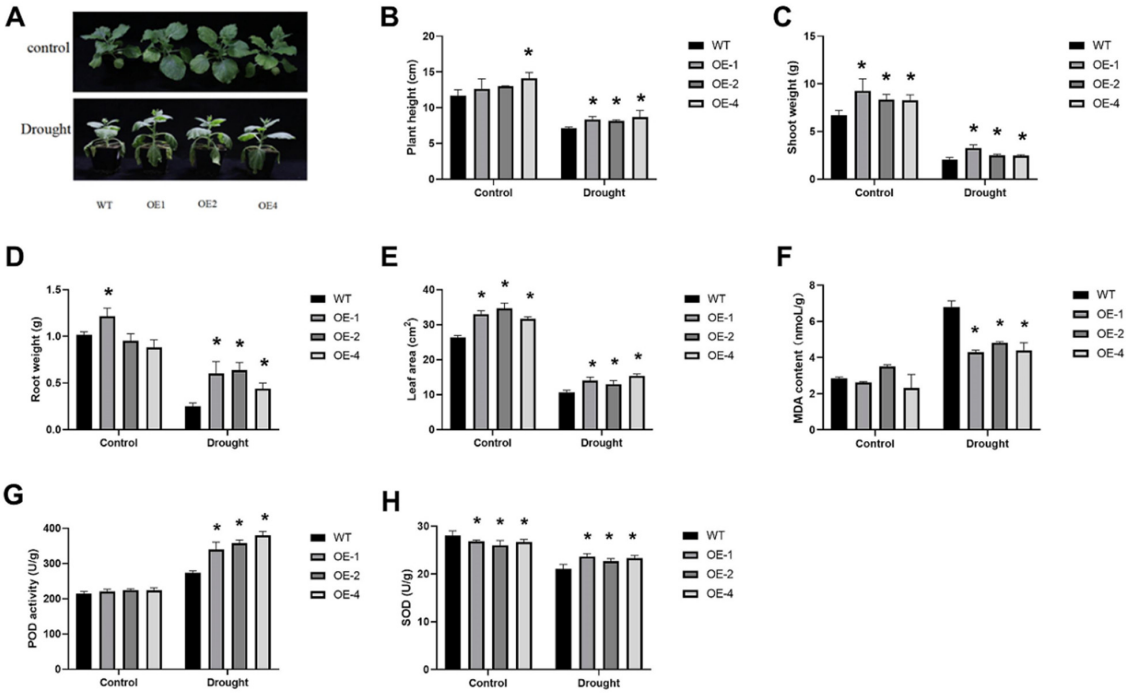

Figure 8. Phenotypic and physiological responses of WT and OE lines to natural drought stress after 7 days of water deprivation. (**A**) Phenotype, (**B**) plant height, (**C**) shoot weight, (**D**) root weight, (**E**) leaf area, (**F**) MDA content, (**G**) POD activity, and (**H**) SOD activity. Data are mean ± SD (n = 5). * $p < 0.05$.

4. Discussion

4.1. ZmXTH23 as a Positive Regulator of Germination Under Stress

Cell wall remodeling proteins, including XTHs, are known to facilitate embryo growth and endosperm weakening during germination. However, their roles under salt stress can be either negative or positive. For instance, *SlXTH1* from *Suaeda liaotungensis* acts as a negative regulator, reducing germination under salt stress through increased XET activity and cell wall tightening [24]. In contrast, our study shows that *ZmXTH23* acts as a positive regulator, enabling >50% germination under 120 mM NaCl. The mechanism may involve a moderate loosening of the cell wall that allows radicle protrusion without compromising structural integrity, but this hypothesis requires direct testing.

4.2. Growth Promotion Under Normal Conditions: Cell Wall Plasticity

Overexpression of *ZmXTH23* increased plant height, root length, and shoot fresh weight under well-watered conditions. This is consistent with the function of other *XTHs*, such as *PcBRU1* in pear, which promotes stem elongation by loosening cell walls [25], and *SlXTH19* in tomato, which increases cell size and wall component deposition [26]. The sequence of ZmXTH23 contains the conserved DEIDFEFLG motif characteristic of XET activity (predicted by homology to AtXTH9), suggesting that it primarily catalyzes xyloglucan transglycosylation rather than hydrolysis. XET activity could rearrange xyloglucan–cellulose cross-links, increasing wall extensibility and thus facilitating cell expansion. This explains the enhanced growth in the OE lines.

4.3. Mechanisms of Stress Tolerance: Antioxidant Upregulation and Water Retention

Under both salt and drought stress, the OE lines exhibited higher SOD and POD activities, lower MDA levels, and increased RWCs compared to the WT plants. Abiotic stress triggers the production of reactive oxygen species (ROS), which induce membrane lipid per-

oxidation as reflected by MDA accumulation. The elevated antioxidant enzyme activities in the OE lines likely reduce ROS levels, thereby preserving membrane integrity [27,28]. The higher RWC observed in the OE lines suggests improved water conservation, which may result from altered cell wall properties that reduce transpirational water loss or enhance root water uptake [29]. It is, therefore, plausible that *ZmXTH23*-mediated cell wall remodeling influences aquaporin activity or hydraulic conductivity, although this hypothesis requires further experimental validation. Although we have determined the apoplastic localization of *ZmXTH23* under normal conditions, whether abiotic stress conditions (such as high salinity or drought) alter its subcellular distribution remains unknown. Several studies have demonstrated that the localization of certain XTH proteins can be regulated by environmental cues, with stress-inducible XTHs often showing dynamic shuttling between the secretory pathway and the apoplast. Further investigation using stress-treated tissues or osmotic adjustment media combined with live-cell imaging will be required to determine whether *ZmXTH23* undergoes stress-induced redistribution [15].

4.4. Functional Divergence of XTHs and Conservation Between Monocots and Dicots

ZmXTH23 positively regulates stress tolerance, whereas *TaXTH17* negatively regulates it [15]. This divergence may arise from differences in enzymatic preference (XET vs. XEH) or spatiotemporal expression patterns. XET generally loosens the wall, while XEH can fragment xyloglucan and potentially weaken wall structure. Our in silico analysis suggests ZmXTH23 is an XET, which would promote wall remodeling without catastrophic weakening. Furthermore, the fact that a maize XTH functions effectively in a dicot host (*N. benthamiana*) indicates that the xyloglucan structure and XTH substrate recognition are highly conserved between different species, validating the heterologous expression approach.

4.5. Limitations and Future Directions

A key limitation is that the conclusions are based on heterologous expression in *N. benthamiana*; the native function of *ZmXTH23* in maize remains to be confirmed by generating stable transgenic maize lines. Additionally, we did not directly measure XET/XEH activity or cell wall mechanical properties (e.g., elasticity or porosity). Future work should include enzymatic assays, cell wall composition analysis, and testing of *ZmXTH23* overexpression in maize under field conditions.

5. Conclusions

ZmXTH23 localizes to the apoplast in *N. benthamiana*. Overexpression of *ZmXTH23* promotes plant height, root length, and shoot fresh weight under normal conditions and enhances tolerance to salt and drought stress during both germination and vegetative growth. The enhanced tolerance is associated with increased antioxidant enzyme activities and improved water retention. These findings identify *ZmXTH23* as a promising candidate for molecular breeding to improve stress resilience in maize, although validation in maize is necessary before practical application.

Supplementary Materials: The following supporting information can be downloaded at: https://www.mdpi.com/article/10.3390/agronomy16131276/s1. Figure S1: PCR amplification of *ZmXTH23* (A) and double enzyme digestion of PMD19T-ZmXTH23 with *Bam*H I and *Xba* I (B); Figure S2: Identification results of pCambia1300-ZmXTH23 vector; Figure S3: Infection and screening process of Bunsen tobacco leaf; Figure S4: Phenotypic identification of wild-type and knockout lines of maize at three-leaf stage under normal growth conditions; Figure S5: Phenotypes of wild-type and knockout lines of maize after 7 days under normal growth conditions (A), salt stress (B), and drought stress (C).

Author Contributions: Conceptualization, X.G.; methodology, Q.M., F.J. and J.L. (Junhua Li); validation, Y.P., Q.X., J.W. and H.G.; formal analysis, Q.M., F.J. and J.L. (Junhua Li); investigation, Q.M., F.J., J.L. (Junhua Li), Y.P., Q.X., J.W. and H.G.; resources, J.L. (Jun Li), H.L., N.C., X.C. and X.S.; data curation, Q.M., F.J. and J.L. (Junhua Li); writing—original draft preparation, Q.M., F.J. and J.L. (Junhua Li); writing—review and editing, X.G.; visualization, Q.M.; supervision, X.G.; project administration, X.G.; funding acquisition, X.G. All authors have read and agreed to the published version of the manuscript.

Funding: This research was funded by the Shandong Improved Variety Program (grant number 2025LZGC013) and the Shandong Excellent Young Scientists Fund Program (Overseas, 2023HWYQ-094).

Data Availability Statement: The raw data supporting the conclusions of this article will be made available by the authors on request.

Acknowledgments: We thank the Key Laboratory of Major Crop Germplasm Innovation and Application in Qingdao for providing experimental facilities. During the preparation of this manuscript, the authors used DeepSeek-V4 for the purposes of text editing. The authors have reviewed and edited the output and take full responsibility for the content of this publication.

Conflicts of Interest: The authors declare no conflicts of interest.

Abbreviations

CLSM	Confocal laser scanning microscope
MDA	Malondialdehyde
MS medium	Murashige and Skoog medium
OE	Overexpressing
PEG	Polyethylene Glycol
POD	Peroxidase
qRT-PCR	Quantitative reverse transcription PCR
ROS	Reactive oxygen species
RWC	Relative water content
SD	Standard deviation
SOD	Superoxide dismutase
WT	Wild-type
XTH	Xyloglucan endotransglucosylase/hydrolase

References

1. Masson-Delmotte, V.; Zhai, P.; Pörtner, H.-O.; Roberts, D.; Skea, J.; Shukla, P.R. *Global Warming of 1.5 °C*; Cambridge University Press: Cambridge, UK, 2022.
2. Cao, Y.; Zhou, X.; Song, H.; Zhang, M.; Jiang, C. Advances in deciphering salt tolerance mechanism in maize. *Crop J.* **2023**, *11*, 1001–1010. [CrossRef]
3. Liu, S.; Wang, H.; Qin, F. Genetic dissection of drought resistance for trait improvement in crops. *Crop J.* **2023**, *11*, 975–985. [CrossRef]
4. Tian, T.; Wang, S.; Yang, S.; Yang, Z.; Liu, S.; Wang, Y.; Gao, H.; Zhang, S.; Yang, X.; Jiang, C.; et al. Genome assembly and genetic dissection of a prominent drought-resistant maize germplasm. *Nat. Genet.* **2023**, *55*, 496–506. [CrossRef] [PubMed]
5. Liang, X.; Li, J.; Yang, Y.; Jiang, C.; Guo, Y. Designing salt stress-resilient crops: Current progress and future challenges. *J. Integr. Plant Biol.* **2024**, *66*, 303–329. [PubMed]
6. Jardine, K.J.; Dewhirst, R.A.; Som, S.; Lei, J.; Tucker, E.; Young, R.P.; Portillo-Estrada, M.; Gao, Y.; Su, L.; Fares, S.; et al. Cell wall ester modifications and volatile emission signatures of plant response to abiotic stress. *Plant Cell Environ.* **2022**, *45*, 3429–3444. [CrossRef] [PubMed]
7. Zhao, N.; Zhou, Z.; Cui, S.; Zhang, X.; Zhu, S.; Wang, Y.; Zenda, T.; Li, W. Advanced imaging-enabled understanding of cell wall remodeling mechanisms mediating plant drought stress tolerance. *Front. Plant Sci.* **2025**, *16*, 1635078. [CrossRef] [PubMed]
8. Shinohara, N.; Nishitani, K. Cryogenian origin and subsequent diversification of the plant cell-wall enzyme *XTH* family. *Plant Cell Physiol.* **2021**, *62*, 1874–1889. [CrossRef] [PubMed]
9. Ishida, K.; Yokoyama, R. Reconsidering the function of the xyloglucan endotransglucosylase/hydrolase family. *J. Plant Res.* **2022**, *135*, 145–156. [CrossRef] [PubMed]

10. Yang, Z.G.; Zhang, R.; Zhou, Z.C. The XTH gene family in *Schima superba*: Genome-wide identification, expression profiles, and functional interaction network analysis. *Front. Plant Sci.* **2022**, *13*, 13911761. [CrossRef] [PubMed]
11. Fu, W.; Fan, D.; Zhang, Y. Genome-wide identification and characterization of xyloglucan endotransglucosylase/hydrolase gene family in maize (*Zea mays* L.) and the function of *ZmXTH30* in response to drought stress. *Environ. Exp. Bot.* **2024**, *222*, 105744.
12. Zhang, C.; He, M.; Jiang, Z.; Liu, L.; Pu, J.; Zhang, W.; Wang, S.; Xu, F. The Xyloglucan Endotransglucosylase/Hydrolase Gene *XTH22/TCH4* Regulates Plant Growth by Disrupting the Cell Wall Homeostasis in *Arabidopsis* under Boron Deficiency. *Int. J. Mol. Sci.* **2022**, *23*, 1250. [PubMed]
13. Takahashi, D.; Johnson, K.L.; Hao, P.; Tuong, T.; Erban, A.; Sampathkumar, A.; Bacic, A.; Livingston, D.P., 3rd; Kopka, J.; Kuroha, T.; et al. Cell wall modification by the xyloglucan endotransglucosylase/hydrolase *XTH19* influences freezing tolerance after cold and sub-zero acclimation. *Plant Cell Environ.* **2021**, *44*, 915–930. [PubMed]
14. Tatsumi, A.; Nagayama, T.; Teramoto, A.; Nakamura, A.; Yokoyama, R.; Furukawa, J.; Iwai, H. *OsXTH19* overexpression improves aluminum tolerance via xyloglucan reduction in rice root cell wall. *Plants* **2025**, *14*, 1912. [CrossRef] [PubMed]
15. Bi, H.H.; Liu, Z.L.; Liu, S.S.; Qiao, W.C.; Zhang, K.P.; Zhao, M.H.; Wang, D.W. Genome-wide analysis of wheat xyloglucan endotransglucosylase/hydrolase (XTH) gene family revealed *TaXTH17* involved in abiotic stress responses. *BMC Plant Biol.* **2024**, *24*, 640. [PubMed]
16. Zhang, Y.R.; Jiao, F.C.; Li, J.; Pei, Y.H.; Zhao, M.A.; Song, X.Y.; Guo, X.M. Transcriptomic analysis of the maize inbred line Chang7-2 and a large-grain mutant tc19. *BMC Genom.* **2022**, *23*, 4. [CrossRef]
17. Barrs, H.D.; Weatherley, P.E. A re-examination of the relative turgidity technique for estimating water deficits in leaves. *Aust. J. Biol. Sci.* **1962**, *15*, 413–428. [CrossRef]
18. Doyle, J.J.; Doyle, J.L. A rapid DNA isolation procedure for small quantities of fresh leaf tissue. *Phytochem. Bull.* **1987**, *19*, 11–15.
19. Livak, K.J.; Schmittgen, T.D. Analysis of relative gene expression data using real-time quantitative PCR and the $2^{-\Delta\Delta CT}$ Method. *Methods* **2001**, *25*, 402–408. [CrossRef] [PubMed]
20. Heath, R.L.; Packer, L. Photoperoxidation in isolated chloroplasts. I. Kinetics and stoichiometry of fatty acid peroxidation. *Arch. Biochem. Biophys.* **1968**, *125*, 189–198. [PubMed]
21. Giannopolitis, C.N.; Ries, S.K. Superoxide dismutases: I. Occurrence in higher plants. *Plant Physiol.* **1977**, *59*, 309–314. [PubMed]
22. Yokoyama, R.; Nishitani, K. A comprehensive expression analysis of all members of a gene family encoding cell-wall enzymes allowed us to predict cis-regulatory regions involved in cell-wall construction in specific organs of Arabidopsis. *Plant Cell Physiol.* **2001**, *42*, 1025–1033. [PubMed]
23. Ma, Y.S.; Zhang, Y.; Zhang, Z.; He, Z.L.; Xun, C.F.; Wang, X.N.; Chen, Y.Z. Genome-wide identification and characterization of the Xyloglucan endotransglucosylase/hydrolase (XTH) gene family in *Camellia oleifera* and the function of *CoXTH1* during drought stress. *Plants* **2025**, *14*, 3605. [PubMed]
24. Song, J.; Ding, H.; Cheng, N.; Li, X.; Lu, Y.; Wang, H.; Li, C.; Li, Q. *SlXTH1*, a xyloglucan endotransglucosylase/hydrolase in halophyte *Suaeda liaotungensis*, negatively regulates *Arabidopsis* seed germination under salt stress. *Plant Sci.* **2025**, *359*, 112672. [PubMed]
25. Li, Y.; Zheng, X.; Wang, C.; Hou, D.; Li, T.; Li, D.; Ma, C.; Sun, Z.; Tian, Y. Pear xyloglucan endotransglucosylase/hydrolases *PcBRU1* promotes stem growth through regulating cell wall elongation. *Plant Sci.* **2021**, *312*, 111026. [PubMed]
26. Luo, J.; Wang, X.; Pang, W.; Jiang, J. GA3-induced *SlXTH19* expression enhances cell wall remodeling and plant height in tomatoes. *Plants* **2024**, *13*, 3578. [PubMed]
27. Miller, G.; Suzuki, N.; Ciftci-Yilmaz, S.; Mittler, R. Reactive oxygen species homeostasis and signalling during drought and salinity stresses. *Plant Cell Environ.* **2010**, *33*, 453–467. [CrossRef] [PubMed]
28. Sairam, R.K.; Tyagi, A.K. ROS and oxidative stress: Origin, cell damage, and role of antioxidants in the cellular defense. *Curr. Sci.* **2004**, *87*, 40–47.
29. Blum, A. Plant water stress, hydraulics, and drought tolerance. *Curr. Opin. Plant Biol.* **2017**, *39*, 21–28.